第 34 卷第 1 期
2018 年 1 月

无 机 化 学 学 报
CHINESE JOURNAL OF INORGANIC CHEMISTRY

Vol.34 No.1
161-169

镉/铅超分子配合物的合成、晶体结构及理论计算

刘 宏[1] 李传碧*,[2] 李国峰[2] 李秀梅[3] 潘亚茹[3]

([1]吉林师范大学信息技术学院,四平 136000)

([2]吉林师范大学环境友好材料制备与应用教育部重点实验室(省部共建),四平 136000)

([3]通化师范学院化学学院,通化 134002)

摘要:通过水热法合成了 2 个新的金属-有机超分子配合物$[CdCl_2(L_1)]_n$ (**1**)和$[Pb(BDC)_{0.5}(HBDC)(L_2)]\cdot 2H_2O$ (**2**)(H_2BDC=对苯二甲酸,L_1=2-(4-氨基苯酚)-1*H*-咪唑并[4,5-f]菲咯啉,L_2=2-(4-*N*,*N*′-二甲基苯)-1*H*-咪唑并[4,5-*f*]菲咯啉)。并对其进行了元素分析、红外光谱、热重、荧光光谱和 X 射线单晶衍射测定。配合物 **1** 是一维链状结构,配合物 **2** 为零维结构,它们均通过氢键和 π-π 堆积形成了三维超分子结构。此外,还用高斯 09 程序 PBE0/LANL2DZ 方法对配合物 **1** 和 **2** 进行了自然键轨道(NBO)分析,计算结果表明配位原子与 Cd(Ⅱ)、Pb(Ⅱ)离子之间存在着共价作用。

关键词:水热合成;晶体结构;镉配合物;铅配合物;自然键轨道

中图分类号:O614.24+2;O614.43+3 **文献标识码**:A **文章编号**:1001-4861(2018)01-0161-09

DOI:10.11862/CJIC.2018.003

Syntheses, Crystal Structures and Theoretical Calculation of Cadmium/Lead Supramolecular Coordination Compounds

LIU Hong[1] LI Chuan-Bi*,[2] LI Guo-Feng[2] LI Xiu-Mei[3] PAN Ya-Ru[3]

([1]*College of Information & Technology, Jilin Normal University, Siping, Jilin* 136000, *China*)

([2]*Key Laboratory of Preparation and Applications of Environmental Friendly Materials, Ministry of Education, Jilin Normal University, Siping, Jilin* 136000, *China*)

([3]*Faculty of Chemistry, Tonghua Normal University, Tonghua, Jilin* 134002, *China*)

Abstract: Two new metal-organic supramolecular coordination compounds $[CdCl_2(L_1)]_n$ (**1**) and $[Pb(BDC)_{0.5}(HBDC)(L_2)]\cdot 2H_2O$ (**2**) (H_2BDC=terephthalic acid, L_1=2-(4-aminophenol)-1*H*-imidazo[4,5-*f*][1,10]phenanthroline, L_2=2-(4-*N*,*N*′-dimethylbenzene)-1*H*-imidazo[4,5-*f*][1,10]phenanthroline) have been hydrothermally synthesized and structurally characterized by elemental analysis, IR spectrum, TG, fluorescence spectrum and single-crystal X-ray diffraction. Complex **1** is one-dimensional chain-like structure, and complex **2** exhibits zero-dimensional framework. They all display three-dimensional supramolecular network via hydrogen bonding and π-π stacking interactions. In addition, we analyzed natural bond orbital (NBO) of **1** and **2** in using the PBE0/LANL2DZ method built in Gaussian09 program. The calculation results showed the obvious covalent interaction between the coordinated atoms and Cd(Ⅱ), Pb(Ⅱ) ion. CCDC: 1472404, **1**; 1551304, **2**.

Keywords: hydrothermal synthesis; crystal structure; cadmium complex; lead complex; natural bond orbital

收稿日期:2017-05-21。收修改稿日期:2017-11-07。

吉林省科技发展计划(No.201205080)资助项目。

*通信联系人。E-mail:lcblh2017@163.com

0 Introduction

Metallosupramolecular species assembled from transition metals and organic bridging ligands with new structures and properties have been rapidly developed due to their interesting structural diversity and potential applications as functional materials[1-5]. However, the reasonable design of new materials for special applications is still attractive. During the past years, several types of forces, such as coordination bonding[6-8], hydrogen bonding[9-11], and π-π stacking[12-13] have been well used in constructing extended supramolecular networks. Up to now, the most important driving forces in crystal engineering are coordination, hydrogen-bonding and π-π stacking interactions, and many networks assembled from mono- or polynuclear metal complexes via hydrogen bonding, π-π stacking interactions were reported recently[14-16]. The unique strength, directionality and complementary of such non-covalent interactions play key roles in the construction of various architectures for molecular self-assembly and recognition[17-19].

Based on all the aspects stated above, herein we report the synthesis and crystal structure of two coordination supramolecule, $[CdCl_2(L_1)]_n$ (**1**) and $[Pb(BDC)_{0.5}(HBDC)(L_2)]\cdot 2H_2O$ (**2**). In the solid state, complexes **1** and **2** form a novel three-dimensional (3D) network resulted from intermolecular hydrogen-bonding and π-π stacking interactions.

1 Experimental

1.1 General procedures

All reagents were purchased commercially and used without further purification. Elemental analyses (C, H and N) were measured on a Vario EL Ⅲ Elemental Analyzer. IR spectrum was recorded in the range of 4 000~400 cm^{-1} on a Nicolet 6700 spectrometer using a KBr pellet. TG studies were carried on a STA7300 analyzer under nitrogen at a heating rate of 10 ℃·min^{-1}. The fluorescent spectrum was obtained on a computer-controlled JY Fluoro-Max-3 spectrometer at room temperature. The power X-ray diffraction (PXRD) studies were performed with a Bruker D8 Discover instrument (Cu $K\alpha$ radiation, λ=0.154 184 nm, U=40 kV, I=40 mA) over the 2θ range of 5°~50° at room temperature.

1.2 Synthesis

$[CdCl_2(L_1)]_n$ (**1**). A mixture of L_1 (0.065 g, 0.2 mmol), $CdCl_2\cdot 2.5H_2O$ (0.091 g, 0.4 mmol) and 18 mL H_2O was adjust pH=6 with 40% NaOH, sealed in a Teflon-lined stainless steel vessel, heated to 140 ℃ for 3 days, and followed by slow cooling (a descent rate of 5 ℃·h^{-1}) to room temperature. Yellow block crystals were obtained. Yield: 53%. Anal. Calcd. For $C_{19}H_{13}CdCl_2N_5O$(%): C, 44.69; H, 2.57; N, 13.71. Found(%): C, 44.05; H, 2.14; N, 13.02. IR (cm^{-1}): 3 043w, 1 610w, 1 584m, 1 457m, 1 346m, 1 136s, 839w, 811w, 732w, 619w, 514w.

$[Pb(BDC)_{0.5}(HBDC)(L_2)]\cdot 2H_2O$ (**2**). A mixture of L_2 (0.068 g, 0.2 mmol), $Pb(NO_3)_2$ (0.066 g, 0.2 mmol), H_2BDC (0.033 g, 0.2 mmol), and 18 mL H_2O was adjust to pH=7 with 40% NaOH, sealed in a Teflon-lined stainless steel vessel, heated to 150 ℃ for 5 days, and followed by slow cooling (a descent rate of 5 ℃·h^{-1}) to room temperature. Colorless block crystals were obtained. Yield: 48%. Anal. Calcd. For $C_{66}H_{52}N_{10}O_{14}Pb_2$(%): C, 48.82; H, 3.23; N, 8.63. Found(%): C, 48.05; H, 2.93; N, 8.01. IR (cm^{-1}): 3 419w, 1 695m, 1 625w, 1 548s, 1 585w, 1 511m, 1 377s, 1 260m, 1 148w, 1 015m, 945m, 875w, 750m, 735w, 643w, 514w.

1.3 Structure determination

Single-crystal X-ray diffraction data for **1** and **2** were recorded on a Bruker D8 QUEST CMOS diffractometer with graphite-monochromated Mo $K\alpha$ radiation (λ=0.071 073 nm) at 293 K. The structure was solved with the direct method of SHELXS-97 and refined with full-matrix least-squares techniques using the SHELXL-97 program[20-21]. The non-hydrogen atoms of the complexes were refined with anisotropic temperature parameters. The hydrogen atoms attached to carbons were generated geometrically. Crystallographic parameters and the data collection statistics for complexes **1** and **2** are given in Table 1. Selected bond lengths and bond angles are listed in Table 2.

CCDC: 1472404, **1**; 1551304, **2**.

Table 1　Crystal data and structure refinement for 1 and 2

Formula	$C_{19}H_{13}CdCl_2N_5O$	$C_{66}H_{52}N_{10}O_{14}Pb_2$
Formula weight	510.64	1623.56
Crystal system	Monoclinic	Monoclinic
Space group	*C*2/*c*	*C*2/*c*
a / nm	2.692 0(4)	1.440 7(5)
b / nm	1.020 82(17)	1.926 0(6)
c / nm	1.432 9(2)	2.182 5(7)
β / (°)	115.159(2)	96.010(5)
Volume / nm^3	3.564 1(10)	6.023(3)
Z	8	4
D_c / (g·cm^{-3})	1.903	1.791
θ range / (°)	1.67~26.15	1.77~25.95
F(000)	2 016	3 176
Reflection collected, unique	9 568, 3 548	16 185, 5 889
Goodness-of-fit on F^2	1.037	1.028
R_{int}	0.021 3	0.033 6
R_1, wR_2 [$I>2\sigma(I)$]	0.027 7, 0.067 9	0.029 0, 0.068 3

Table 2　Selected bond lengths (nm) and bond angles (°) for 1 and 2

		1			
Cd(1)-N(1)	0.232 1(2)	Cd(1)-N(2)	0.233 6(2)	Cd(1)-N(5^{i})	0.255 4(3)
Cd(1)-Cl(1)	0.258 96(9)	Cd(1)-Cl(2)	0.258 65(8)	Cd(1)-Cl(2^{ii})	0.258 16(8)
N(1)-Cd(1)-N(2)	71.44(8)	N(1)-Cd(1)-N(5^{ii})	87.30(8)	N(2)-Cd(1)-N(5^{ii})	86.53(8)
N(1)-Cd(1)-Cl(2^{ii})	164.68(6	N(2)-Cd(1)-Cl(2^{ii})	95.59(6)	O(7)-Cd(1)-O(2)	92.08(6)
N(1)-Cd(1)-Cl(2)	98.19(6)	N(2)-Cd(1)-Cl(2)	166.30(6)	N(5^{i})-Cd(1)-Cl(2)	84.00(6)
Cl(2^{ii})-Cd(1)-Cl(2)	93.18(2)	N(1)-Cd(1)-Cl(1)	95.11(6)	N(2)-Cd(1)-Cl(1)	96.22(6)
N(5^{i})-Cd(1)-Cl(1)	176.81(6)	Cl(2^{ii})-Cd(1)-Cl(1)	94.38(3)	Cl(2)-Cd(1)-Cl(1)	93.57(3)
		2			
Pb(1)-O(1)	0.266 8(4)	Pb(1)-O(2)	0.258 8(3)	Pb(1)-O(1W)	0.262 9(3)
Pb(1)-O(6)	0.236 3(3)	Pb(1)-N(1)	0.262 3(4)	Pb(1)-N(2)	0.256 5(3)
O(6)-Pb(1)-N(2)	82.07(11)	O(6)-Pb(1)-O(2)	82.52(12)	N(2)-Pb(1)-O(2)	80.44(11)
O(6)-Pb(1)-N(1)	82.32(12)	N(2)-Pb(1)-N(1)	63.67(11)	O(2)-Pb(1)-N(1)	142.56(11)
O(6)-Pb(1)-O(5)	52.24(10)	N(2)-Pb(1)-O(5)	126.17(11)	O(2)-Pb(1)-O(5)	114.54(12)
N(1)-Pb(1)-O(5)	81.50(11)	O(6)-Pb(1)-O(1)	80.03(13)	N(2)-Pb(1)-O(1)	128.48(11)
O(2)-Pb(1)-O(1)	49.59(10)	N(1)-Pb(1)-O(1)	156.34(13)	O(5)-Pb(1)-O(1)	75.26(12)

Symmetry codes: ^{i} 2−*x*, 1−*y*, 2−*z*; ^{ii} −*x*+3/2, −*y*+1/2, 1−*z*.

2　Results and discussion

2.1　IR spectrum

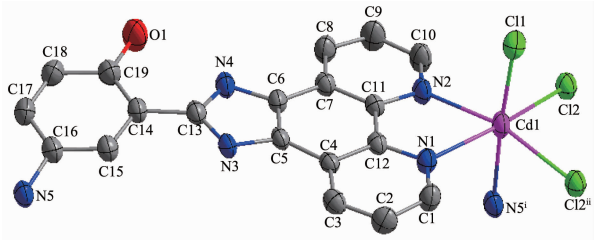
In the IR spectrum of complex **1**, the C-H stretching mode for the phenyl ring is relatively weak and observed at about 3 043 cm^{-1}. Peaks at 1 610, 1 584 and 1 457 cm^{-1} could belong to ν(C=C) vibration of aromatic ring. The peak at 1 346 cm^{-1} is ascribed to the ν(C=N) vibration of L_1.

In the IR spectra of the complex **2**, $\nu_{as}(CO_2)$ and $\nu_s(CO_2)$ stretching vibrations at 1 548 and 1 377 cm^{-1} show that the BDC^{2-} ligand adopts bidentate and

chelating coordination modes. A strong band at 1 695 cm^{-1} is assigned to the protonated carboxylic group[22]. The spectrum also exhibits one intense broad band with the frequency of 3 419 cm^{-1}, which can be assigned to the stretching vibration of crystal water molecule[23].

2.2 Description of the structure

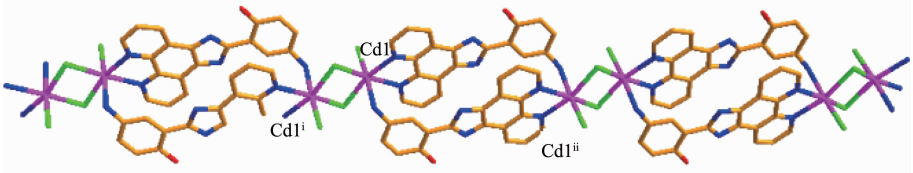
X-ray crystallography reveals that complex **1** consists of one Cd(Ⅱ) ion, one L_1 ligand and two chloride ions in each independent crystallographic unit. The ORTEP view of complex **1** with atom labeling is shown in Fig.1. The coordination geometry around the Cd(Ⅱ) center could be described as a distorted octahedral environment generated by Cl(2)-Cl(2B)-N(1)-N(2) consisting of the basal plane, and one chloride ion (Cl(1)), one nitrogen atom (N(5A)) occupying the axial positions from the opposite direction. The bond distances of Cd-N in complex **1** fall in the range of 0.232 1(2)~0.255 4(3) nm, and those of Cd-Cl in 0.258 65(8)~0.258 96(9) nm. The coordination angles around the Cd atom vary from 71.44(8)° to 176.81(6)°.



H atoms were omitted for clarity; Ellipsoids at 30% probability; Symmetry codes: [i] 2–*x*, 1–*y*, 2–*z*; [ii] –*x*+3/2, –*y*+1/2, 1–*z*

Fig.1 ORTEP view of complex **1** with atom labeling

In **1**, two chloride ions take μ_2 bridging mode and each L_1 ligand adopts μ_3 coordination fashion to bridge Cd(Ⅱ) ions into an infinite one-dimensional double-chain, which contains 4-membered rings and 28-membered rings in turn with Cd⋯Cd distances of 0.355 1 and 1.251 5 nm, respectively (Fig.2). Further investigation of the crystal packing of complex **1** shows that there are O–H⋯N, C–H⋯O, C–H⋯Cl and N–H⋯Cl hydrogen bonding interactions between hydroxyl oxygen atom, nitrogen atom, carbon atoms of L_1 ligands and chloride ions (Table 3), as shown in



Symmetry codes: [i] 2–*x*, 1–*y*, 2–*z*; [ii] 1–*x*, –*y*, 1–*z*

Fig.2 View of the one-dimensional double-chain structure in **1**

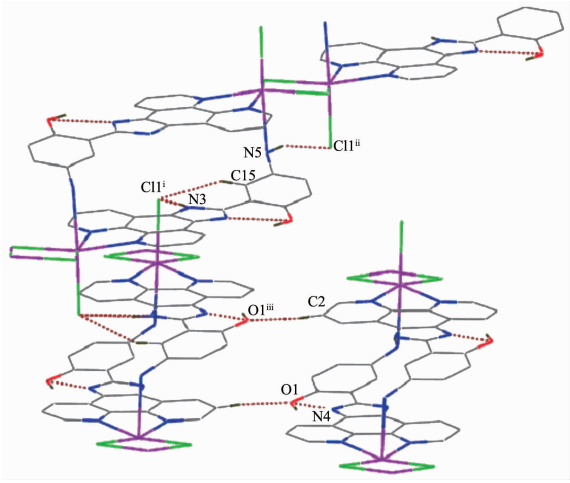
Table 3 Hydrogen bonds for complex 1 and 2

D–H⋯A	*d*(D-H) / nm	*d*(H⋯A) / nm	*d*(D⋯A) / nm	∠DHA / (°)
		1		
O(1)–H(1A)⋯N(4)	0.082	0.189	0.261 4(4)	146
N(3)–H(3A)⋯Cl(1)[i]	0.085(3)	0.233(3)	0.318 1(3)	173(3)
N(5)–H(5B)⋯Cl(1)[ii]	0.086	0.261	0.341 6(3)	157
C(2)–H(2)⋯O(1)[iii]	0.094(3)	0.254(3)	0.332 0(4)	140(3)
C(15)–H(15)⋯Cl(1)[iii]	0.107(3)	0.266(3)	0.366 1(3)	156(2)
		2		
O(3)–H(3A)⋯O(4)[i]	0.082	0.185 5	0.266 1	167
O(7)–H(7B)⋯O(1)[ii]	0.085	0.225 4	0.273 6	116
N(3)–H(3B)⋯O(6)[iii]	0.086	0.226 7	0.306 1	154
O(7)–H(7D)⋯N(4)[iv]	0.085	0.225 4	0.273 6	141

Symmetry codes: [i] –*x*, *y*, 1/2–*z*; [ii] 1/2–*x*, 3/2–*y*, 1–*z*; [iii] *x*, 1+*y*, *z* for **1**; [i] –*x*+3, –*y*+1, –*z*+1, [ii] –*x*+2, *y*, –*z*+1/2, [iii] –*x*+1, *y*, –*z*+1/2, [iv] *x*+1/2, *y*–1/2, *z* for **2**.

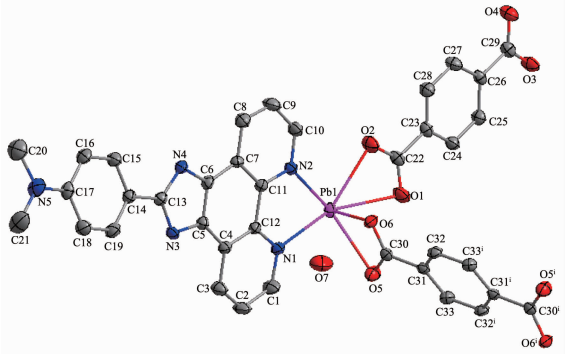
Fig.3. In addition, there are π-π interactions in complex **1** between 5-membered rings and 6-membered rings of L_1 ligands. The most shortest distance between ring centroids is 0.348 91(18) nm and dihedral angle is 2° (Table 4). As a result, the one-dimensional double-chains are further extended into a three-dimensional supramolecular architecture through hydrogen bonds and π-π interactions.

The structure of complex **2** consists of one Pb(Ⅱ) ion, half BDC^{2-} ligand, one $HBDC^-$ ligand, one L_2 molecule and two lattice water molecule. The ORTEP view of complex **2** with atom labeling is shown in Fig. 4. In this complex, half ligand BDC^{2-} takes the unusual bi-deprotonated BDC^{2-} form, and adopts bidentate coordination mode using two oxygen atoms of two carboxylate groups, one ligand takes di-protonated $HBDC^-$ form, and adopts bidentate coordination mode using two oxygen atoms of one carboxylate group. The ligand L_2 chelates with the Pb(Ⅱ) center to result in pentangular pyramid environment. The Pb-N and Pb-O bond distances lie in the range of 0.256 5(3) ~0.262 3(4) nm and 0.236 3(3)~0.266 8(4) nm,



Symmetry codes: i −x, y, 1/2−z; ii 1/2−x, 3/2−y, 1−z; iii x, 1+y, z

Fig.3　View of hydrogen-bonding interactions of **1**



H atoms were omitted for clarity; Ellipsoids at 30% probability; Symmetry codes: i 3/2−x, 1/2−y, 1−z

Fig.4　ORTEP view of complex **2** with atom labeling

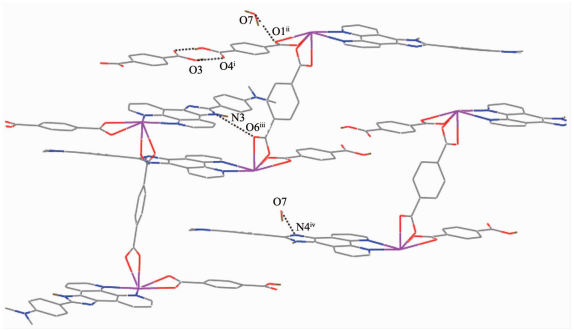
Table 4　Parameters between the planes in 1 and 2

Plane	Distance between ring centroids /nm	Dihedral angle / (°)	Perpendicular distance of plane(*I*) on ring(*J*) / nm	Perpendicular distance of plane(*J*) on ring(*I*) / nm
		1		
Plane(3)→Plane(5)^{i}	0.363 0(2)	3.26(16)	0.332 84(12)	0.336 51(13)
Plane(3)→Plane(6)^{i}	0.353 78(17)	1.30(15)	0.331 88(12)	0.331 15(11)
Plane(4)→Plane(4)^{i}	0.349 2(2)	1	0.329 70(13)	0.329 70(13)
Plane(4)→Plane(7)^{ii}	0.358 9(2)	9.00(16)	−0.325 98(13)	−0.322 12(14)
Plane(5)→Plane(3)^{i}	0.363 0(2)	3.26(16)	0.336 51(13)	0.332 84(12)
Plane(6)→Plane(3)^{i}	0.353 77(17)	1.30(15)	0.331 15(11)	0.331 88(12)
Plane(6)→Plane(6)^{i}	0.348 91(18)	2	0.330 81(11)	0.330 81(11)
Plane(7)→Plane(4)^{ii}	0.358 9(2)	9.00(16)	−0.322 12(14)	−0.325 98(13)
		2		
Plane(1)→Plane(3)^{iii}	0.361 1(3)	6.1(2)	0.342 68(18)	0.346 12(19)
Plane(1)→Plane(4)^{iii}	0.370 7(3)	3.2(2)	0.342 32(18)	0.338 69(18)
Plane(2)→Plane(2)^{iii}	0.362 3(3)	4	0.344 5(2)	0.344 5(2)
Plane(3)→Plane(6)^{iv}	0.380 2(3)	1.8(2)	−0.345 23(19)	−0.350 01(18)
Plane(4)→Plane(4)^{iv}	0.349 6(3)	3	0.339 81(17)	0.339 81(17)
Plane(5)→Plane(6)^{v}	0.375 2(3)	9.9(2)	0.345 56(19)	−0.359 25(18)

Symmetry codes: i 2−x, y, 3/2−z; ii 2−x, 1−y, 2−z for **1**; iii 1−x, y, 1/2−z; iv 2−x, y, 1/2−z; v −1+x, 1−y, −1/2+z for **2**.

respectively, all being normal for such coordination bonds.

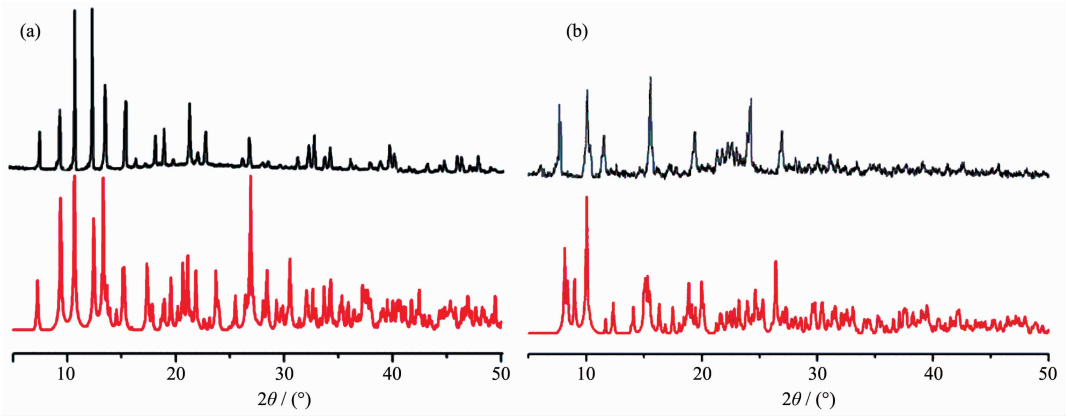
Further investigation of the crystal packing of complex **2** suggests that there are persistent O–H···O, N–H···O and O–H···N hydrogen bonding interactions (Fig.5) between carboxylate oxygen atoms, nitrogen atom of L_2 ligands and crystal water molecules (Table 3) and are usually important in the synthesis of supramolecular architecture. Moreover, there are π-π interactions in complex **2** between imidazole rings, pyridine rings, benzene rings of L_2 ligands and between benzene rings of $HBDC^-$ ligands. The most shortest distance between ring centroids is 0.349 6(3) nm and dihedral angle is 3° (Table 4). Therefore, through hydrogen bonds and π-π interactions, complex **2** is further extended into a two-dimensional supramolecular network framework.



Symmetry codes: [i] $-x+3, -y+1, -z+1$; [ii] $-x+2, y, -z+1/2$; [iii] $-x+1, y, -z+1/2$; [iv] $x+1/2, y-1/2, z$

Fig.5 View of hydrogen-bonding interactions of **2**

To confirm the phase purity of complex **1** and **2**, powder X-ray diffraction (PXRD) patterns were recorded for **1** and **2**, and they were comparable to the corresponding simulated patterns calculated from the single-crystal diffraction data (Fig.6), indicating a pure phase of bulky sample.



Bottom: simulated; Top: experimental

Fig.6 PXRD analysis of the title complex **1** (a) and **2** (b)

2.3 Photoluminescent properties

Luminescence property is very significant in photochemistry and photophysics[24-25]. So in this study, we measured the solid-state photoluminescence spectra of **1** and **2** (Fig.7) at room temperature. Excited by 325 nm, complex **1** exhibits blue emission with the maximum peak at 435 nm. Complex **2** gives green photoluminescence with an emission maximum at 546 nm upon excitation at 325 nm. In order to study the nature of these emission bands, we first analyzed the photoluminescence properties of free L_1, L_2, H_2BDC ligands, and confirmed that they do not emit any luminescence in the range of 400~800 nm. Therefore, on the basis of the previous literature[26], the emission band could be vested to the emission of ligand-to-metal charge transfer (LMCT). For possessing strong fluorescent intensity, it seems to be good candidates for novel hybrid inorganic-organic photoactive materials.

2.4 Theoretical calculation

All calculations in this work were carried out with the Gaussian09 program[27]. The parameters of the molecular structure for calculation were all from the experimental data of the complex. Natural bond orbital (NBO) analysis was performed by density functional theory (DFT)[28] with the PBE0[29] hybrid

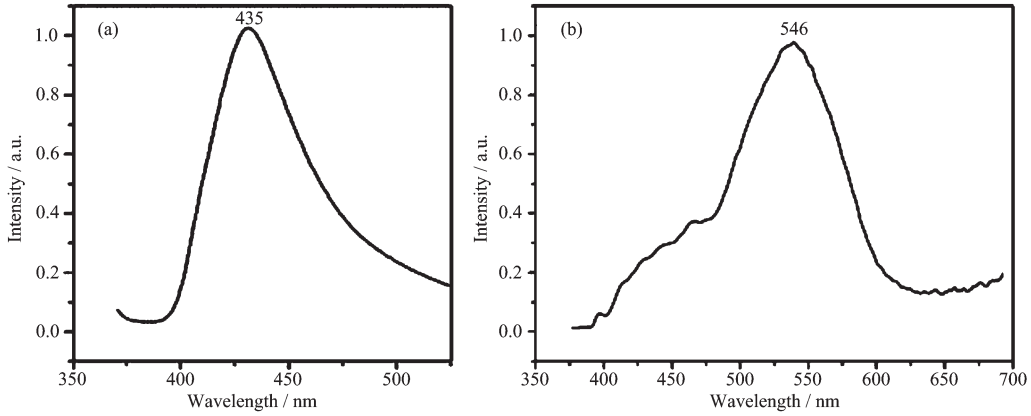


Fig.7　Solid-state emission spectra of **1** (a) and **2** (b) at room temperature

functional and the LANL2DZ basis set[30].

The selected natural atomic charges, natural electron configuration, Wiberg bond indices and NBO bond orders for the compound **1** are displayed in Table 5. The electronic configurations of Cd(1) ion, N and Cl atoms are $5s^{0.40}4d^{9.99}5p^{0.44}$, $2s^{1.22\sim1.34}2p^{4.17\sim4.55}$ and $3s^{1.83\sim1.93}3p^{5.42\sim5.79}$, respectively. In view of the above effects, one can infer that the Cd(1) ion coordination with N and Cl atoms is mainly on 4*d*, 5*s*, and 5*p* orbitals. Nitrogen atoms form coordination bonds with Cd(1) ion using 2*s* and 2*p* orbitals. All Cl atoms provide electrons of 3*s* and 3*p* to Cd(1) ion and form the coordination bonds. Therefore, the Cd(1) ion gained some electrons from three nitrogen atoms of L_1 ligand, three Cl atoms[30-31]. So, on the basis of valence-bond theory, the atomic net charge distribution and the NBO bond orders of the complex **1** (Table 5) exhibits the obvious covalent interaction between the coordinated atoms and Cd(1) ion. The differences of the NBO bond orders for Cd-Cl and Cd-N bonds make their bond lengths be different[31], which are in good agreement with the X-ray crystal structural data of complex **1**.

As can be seen from the Fig.8, lowest unoccupied molecular orbital (LUMO) is mainly consists of L_1 ligand, whereas highest occupied

Table 5　Natural atomic charges, natural valence electron configuration, Wiberg bond indexes and NBO bond orders for 1 and 2

Atom	Net charge	Electron configuration	Bond	Wiberg bond index	NBO bond order / a.u.
		1			
Cd(1)	1.154 95	[core]5*s*(0.40)4*d*(9.99)5*p*(0.44)			
N(1)	−0.515 35	[core]2*s*(1.32)2*p*(4.17)	Cd(1)-N(1)	0.146 5	0.214 1
N(2)	−0.529 22	[core]2*s*(1.34)2*p*(4.18)	Cd(1)-N(2)	0.130 3	0.201 0
N(5)i	−0.789 70	[core]2*s*(1.22)2*p*(4.55)	Cd(1)-N(5)^{i}	0.080 7	0.127 8
Cl(1)	−0.714 67	[core]3*s*(1.93)3*p*(5.78)	Cd(1)-Cl(1)	0.452 5	0.434 7
Cl(2)	−0.721 34	[core]3*s*(1.93)3*p*(5.79)	Cd(1)-Cl(2)	0.438 8	0.421 7
Cl(2)^{ii}	−0.263 30	[core]3*s*(1.83)3*p*(5.42)	Cd(1)-Cl(2)^{ii}	0.173 7	0.244 6
		2			
Pb(1)	1.401 41	[core]6*s*(1.93)6*p*(0.66)			
O(1)	−0.739 85	[core]2*s*(1.71)2*p*(5.01)	Pb(1)-O(1)	0.150 8	0.121 4
O(2)	−0.776 94	[core]2*s*(1.70)2*p*(5.06)	Pb(1)-O(2)	0.169 3	0.134 7
O(5)	−0.721 43	[core]2*s*(1.71)2*p*(5.00)	Pb(1)-O(5)	0.149 3	0.122 1
O(6)	−0.781 75	[core]2*s*(1.72)2*p*(5.06)	Pb(1)-O(6)	0.234 4	0.180 0
N(1)	−0.501 12	[core]2*s*(1.35)2*p*(4.13)	Pb(1)-N(1)	0.109 4	0.141 2
N(2)	−0.522 75	[core]2*s*(1.35)2*p*(4.16)	Pb(1)-N(2)	0.138 2	0.162 9

molecular orbital (HOMO) mainly composed of L_1 ligand too. So, the charge transfer from ligand to ligand and ligand to metal may be deduced from some contours of molecular orbital of complex **1**.

The selected natural atomic charges, natural electron configuration, Wiberg bonds and NBO bond orders for the complex **2** are shown in Table 5. It is indicated that the electronic configurations of Pb(1) ion, N and O atoms are $6s^{1.93}6p^{0.66}$, $2s^{1.35}2p^{4.13\sim4.16}$ and $2s^{1.70\sim1.72}2p^{5.00\sim5.16}$, respectively. Based on the above results, one can conclude that the Pb(1) ion coordination with N and O atoms is mainly on 6*s* and 6*p* orbitals. N atoms form coordination bonds with Pb(1) ion using 2*s* and 2*p* orbitals. All O atoms supply electrons of 2*s* and 2*p* to Pb(1) ion and form the coordination bonds. Therefore, the Pb(1) ion obtained some electrons from N atoms and O atoms of ligands[30-31]. Thus, according to valence-bond theory, the atomic net charge distribution of the complex **2** shows the obvious covalent interaction between the coordinated atoms and Pb(1) ion.

As can be seen from the Fig.9, LUMO is mainly composed of L_2 ligand, whereas HOMO mainly consists of L2 ligand too. So, ILMT may be inferred from some contours of molecular orbital of complex **2**.

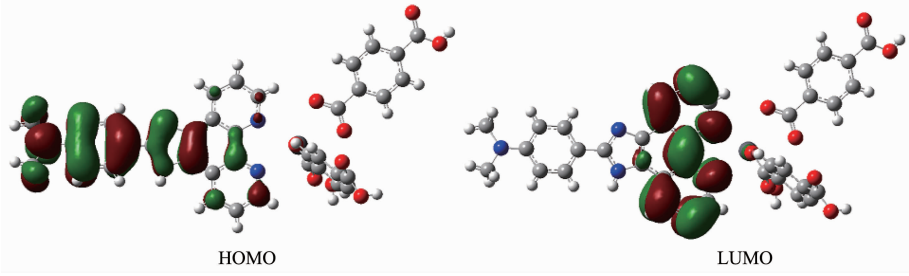


Fig.8 Frontier molecular orbitals of the complex **1**

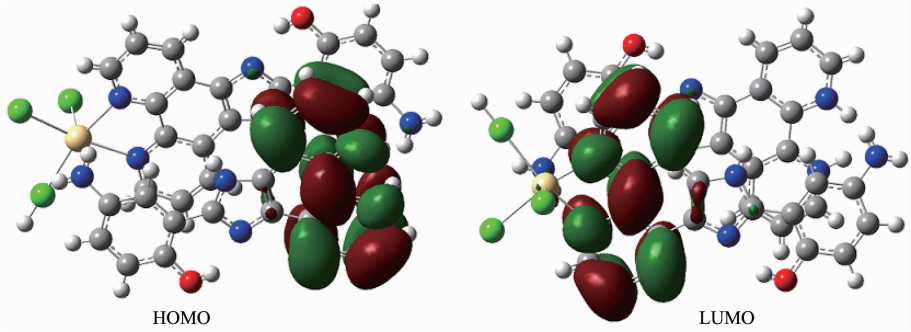


Fig.9 Frontier molecular orbitals of the complex **2**

References:

[1] Wu J F, Zhao L, Zhang L, et al. *Inorg. Chem.*, **2016**,**55**:5514-5519

[2] Du M, Bu X H, Guo Y M, et al. *Chem. Commun.*, **2002**:1478-1479

[3] Ye B H, Tong M L, Chen X M. *Coord. Chem. Rev.*, **2005**, **249**:545-565

[4] WANG Qing-Wei(王庆伟), SUI Wei(隋薇), WANG Ya-Nan (王亚楠), et al. *Chinese J. Inorg. Chem.*(无机化学学报), **2016**,**32**:1120-1126

[5] Evans O R, Lin W B. *Acc. Chem. Res.*, **2002**,**35**:511-522

[6] Yaghi O M, Li G, Li H. *Nature*, **1995**,**378**:703-706

[7] Fujita M, Oka H, Yamaguchi K, et al. *Nature*, **1995**,**378**:469-471

[8] Power K N, Hennigar T L, Zaworotko M J. *Chem. Commun.*, **1998**:595-596

[9] Sadakiyo M, Yamada T, Kitagawa H. *J. Am. Chem. Soc.*, **2011**,**133**:11050-11063

[10]Rigane I, Walha S, Salah A B. *J. Chem. Sci.*, **2016**,**128**: 1395-1404

[11]Juan C M R, Lee B. *Coord. Chem. Rev.*, **1999**,**183**:43-80

[12]Melnic E, Tocana E, Siminel A V, et al. *Polyhedron*, **2015**, **102**:410-416

[13]Tse M C, Cheung K K, Chan M C W, et al. *Chem. Commun.*, **1998**:2295-2296

[14]Li X M, Wang Q W, Zhan P Y, et al. *J. Chem. Crystallogr.*, **2016**,**43**:163-169

[15]Jiang D Y, Sui W, Li X M, et al. *Chin. J. Struct. Chem.*, **2016**,**35**:505-513

[16]Sun Y X, Wang L, Dong X Y, et al. *Synth. React. Inorg. Met.-Org. Nano-Metal Chem.*, **2013**,**43**:599-603

[17]Lehn J M. *Supramolecular Chemistry*. Weinheim: VCH, **1995**.

[18]Whitesides G M, Mathias J P, Seto C T. *Science*, **1991**,**254**: 1312-1319

[19]Rebek J. *Angew. Chem., Int. Ed.*, **1990**,**29**:245-255

[20]Sheldrick G M. *SHELXS*-97, *Program for the Solution of Crystal Structure*, University of Göttingen, Germany **1997**.

[21]Sheldrick G M. *SHELXL*-97, *Program for the Refinement of Crystal Structure*, University of Göttingen, Germany **1997**.

[22]Fu Z Y, Wu X T, Dai J C, et al. *Eur. J. Inorg. Chem.*, **2002**: 2730-2735

[23]Nakomoto K. *Infrared and Raman Spectra of Inorganic and Coordination Compounds*. New York: Wiley, **1986**.

[24]Mizukami S, Houjou H, Sugaya K, et al. *Chem. Mater.*, **2005**, **17**:50-56

[25]Tang C W, Vanslyke S A. *Appl. Phys. Lett.*, **1987**,**51**:913-915

[26]Zheng S L, Chen X M. *Aust. J. Chem.*, **2004**,**57**:703-712

[27]Frisch M J, Trucks G W, Schlegel H B, et al. *Gaussian*09, *Revision B*.09, Gaussian, Inc., Pittsburgh, **2009**.

[28]Parr R G, Yang W. *Density Functional Theory of Atoms and Molecules*. Oxford: Oxford University Press, **1989**.

[29](a)Ernzerhof M, Scuseria G E. *J. Chem. Phys.*, **1999**,**110**: 5029-5036

(b)Adamo C, Barone V. *J. Chem. Phys.*, **1999**,**110**:6158-6170

[30]Wang L, Zhao J, Ni L, et al. *Z. Anorg. Allg. Chem.*, **2012**, **638**:224-230

[31]LI Zhang-Peng(李章朋), XING Yong-Heng(邢永恒), ZHANG Yuan-Hong(张元红), et al. *Acta Phys.-Chim. Sin.*(物理化学学报), **2009**,**25**:741-746